Fractional Ventilation Mapping using Inert Fluorinated Gas MRI in a Rat Model of Inflammation

Marcus J. Couch[1,2], Matthew S. Fox[3,4], Chris Viel[1,2], Gowtham Gajawada[1,2], Tao Li[2], and Mitchell S. Albert[1,2]

[1]Lakehead University, Thunder Bay, Ontario, Canada, [2]Thunder Bay Regional Research Institute, Thunder Bay, Ontario, Canada, [3]Robarts Research Institute, London, Ontario, Canada, [4]Department of Medical Biophysics, Western University, London, Ontario, Canada

Introduction: Interstitial lung disease (ILD) refers to a group of pulmonary disorders that are associated with inflammation and fibrosis in the interstitial tissues between the alveoli and capillary blood (1). ILD typically results in a thickened blood-gas barrier and impaired gas exchange. In many cases the cause of ILD is unknown, and the prognosis is generally very poor. Pre-clinical imaging of animal models of disease may be an important component in understanding the pathophysiology of ILD, as well as in the development of novel therapeutics and diagnostic techniques. In particular, the instillation of the lipopolysaccharide (LPS) (2) or bleomycin (3) in rat lungs has been established as models that mimic inflammation that is similar to ILD. Hyperpolarized (HP) ^{129}Xe MRI is emerging as a useful technique for studying LPS and bleomycin-induced inflammation, as the HP ^{129}Xe can be separately visualized in the lung airspaces, barrier tissues, and red blood cells (RBCs). Cleveland et al. recently demonstrated a reduced ^{129}Xe RBC signal in bleomycin treated rats, which was indicative of reduced gas exchange ability due to fibrotic thickening (3). Unfortunately, HP ^{129}Xe MRI is a technique that has certain disadvantages, which will make translation to routine clinical use difficult. That is, HP ^{129}Xe MRI requires an expensive polarizer, and xenon gas that is enriched with ^{129}Xe isotopes is also very expensive. ^{19}F MRI of the lungs using inert fluorinated gases is a new and promising alternative to HP gas lung MRI. Inert fluorinated gas MRI has the advantages of using gases that are nontoxic, abundant, and inexpensive compared to HP gases. Due to the high gyromagnetic ratio of ^{19}F, there is sufficient thermally polarized signal for imaging, and averaging within a single breath-hold is possible due to short longitudinal relaxation times. Therefore, the gases do not need to be hyperpolarized prior to their use in MRI. Numerous animal studies have been performed using inert fluorinated gas MRI since 1984 (4, 5), and this technique has recently been demonstrated in healthy volunteers (6) and patients with pulmonary diseases (7). In this study, lung imaging was performed using inert fluorinated gas MRI in a rat model of inflammation, and fractional ventilation maps were compared between rats that were instilled with LPS and controls.

Methods: 11 male Sprague Dawley rats (344 ± 26 g) were imaged in this study using an animal care protocol approved by the local animal care committee. 6 rats were instilled with a dose of 2.5 mg/kg LPS two days prior to imaging. The remaining 5 rats were used as controls. Imaging was performed using a 3.0 T Philips Achieva scanner and a home-built linear dual-tuned ^{1}H/^{19}F transmit/receive birdcage coil. Following preparation, rats were ventilated with a mixture of 80% sulfur hexafluoride (SF_6) and 20% O_2 using a custom-built MR-compatible ventilator (8). Fractional ventilation maps were obtained in the axial plane using the method of Ouriadov et al. (9). After at least a 3 minute period of continuous breathing of the SF_6/O_2 mixture, a 10 s breath-hold was initiated for the acquisition of a baseline MR image. Breathing was then switched to pure O_2 for 9 breaths, and a 10 s breath-hold was initiated following each O_2 breath in order to acquire a series of wash-out images. During each breath-hold, a whole-lung 2D projection ^{19}F MR image was obtained in the axial plane using the x-centric pulse sequence (i.e., Cartesian sampling with a partial echo factor of 0.505) with the following settings: TR = 4 ms, TE = 0.48 ms, FOV = 75 x 75 mm^2, matrix = 64 x 64, FA = 70°, BW = 400 Hz/pixel, 65 averages. Since only half of k-space was collected during each wash-out series, the entire wash-out protocol was repeated using the opposite readout gradient polarity in order to create a fully sampled k-space data set for reconstruction. Fully sampled and reconstructed k-space data sets were then averaged 3 times. The final wash-out images were fitted on a pixel-by-pixel basis in Matlab with the following equation:

$$S(n) = const \cdot (1-r)^n$$

where S is the available signal at breath number n, and r is the fractional ventilation, which is defined as the ratio of fresh gas entering a voxel at each breath, divided by the total amount of gas in each voxel:

$$r = \frac{V_{new}}{V_{total}} = \frac{V_{new}}{V_{old} + V_{new}}$$

Rats were euthanized at the end of the experiment, and the lungs were excised and fixed in formalin before being embedded in paraffin. Representative sections were extracted and stained with hematoxylin and eosin for measurement of the alveolar wall thickness.

Results and Discussion: Figure 1 shows two representative series of ^{19}F wash-out images in the axial plane from a control rat and an LPS-instilled rat. In the control rat, the ^{19}F signal is essentially zero by the 5th O_2 wash-out breath, indicating that the gas in the lungs has been completely replaced with O_2. The mean r value from the calculated fractional ventilation map was 0.24 ± 0.04 in this case. For the LPS-instilled rat, the gas in the lungs was been completely replaced with O_2 by the 9th washout breath, with a mean r value of 0.13 ± 0.02. The mean r value for LPS rats was 0.16 ± 0.08, while the mean r value for control rats was 0.20 ± 0.06. These r values agreed with expectations based on the known ventilator settings and expected lung size [TV = 7 mL/kg, FRC = 8 mL, r = TV / (TV + FRC) = 0.23]. Overall, there was a trend towards decreased r values in LPS rats compared to controls, however, this trend was not statistically significant (p = 0.40).

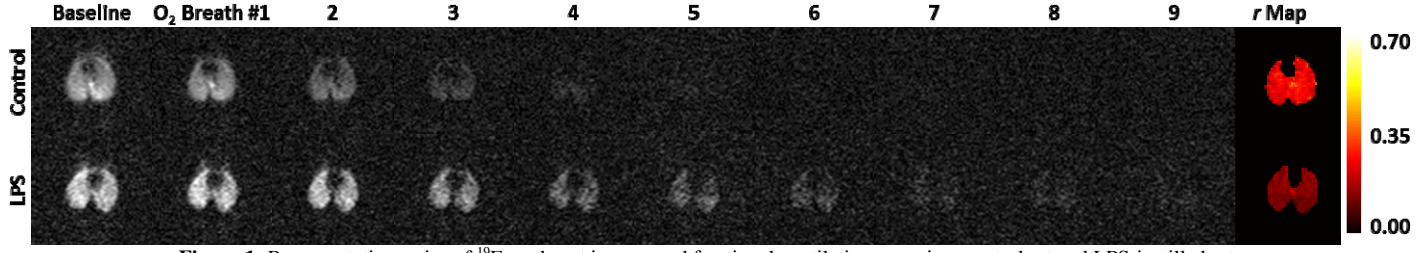

Figure 1: Representative series of ^{19}F wash-out images and fractional ventilation maps in a control rat and LPS-instilled rat.

Fractional ventilation gradients were calculated in the anterior/posterior (A/P) direction from axial fractional ventilation maps. Representative gradients from a control rat and an LPS-instilled rat are shown in Figure 2. Overall, the ventilation gradients calculated from control and LPS-instilled rats were statistically different (p = 0.0001). The mean ventilation gradient for control rats had a slope of -0.008 ± 0.006 cm^{-1}, while the mean ventilation gradient for LPS-instilled rats had a slope of 0.012 ± 0.004 cm^{-1}. Ventilation gradients from control rats agree with expectations, where ventilation is greatest in more dependent regions of the lung, and there is a gravitational gradient due to a gradient in lung compliance. Ventilation gradients from LPS-instilled rats had a positive slope, and this result may be explained by a decrease in lung compliance in dependent regions of the lung due to the presence of inflammation and fibrosis. The micrographs shown in Figure 2 confirm that the alveolar wall thickness is elevated in LPS-instilled rats compared to controls (400x magnification). The mean alveolar wall thickness for LPS-instilled rats was 0.012 ± 0.003 mm, while the mean alveolar wall thickness for control rats was 0.006 ± 0.001 mm (p = 0.0094).

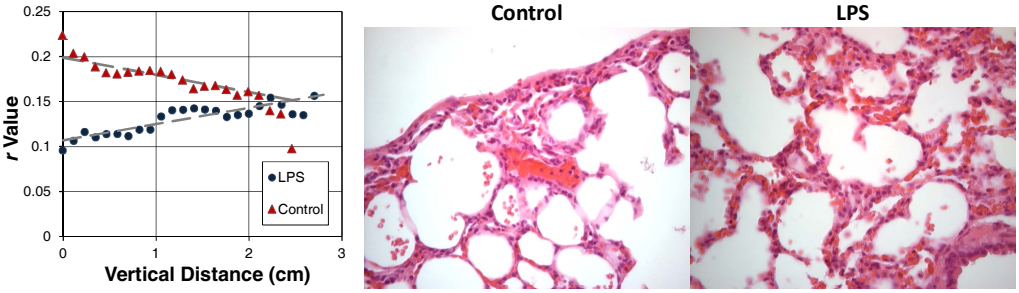

Figure 2: (left) Representative ventilation gradients calculated in the anterior/posterior (A/P) direction from a control rat and LPS-instilled rat. (right) Representative micrographs from a control rat and an LPS-instilled rat.

Conclusions: To our knowledge, this is the first demonstration of inert fluorinated gas MRI in an LPS-instilled model of inflammation in rats. This work demonstrates the potential for inert fluorinated gas MRI to detect the presence of inflammation using a simple and inexpensive approach that can potentially be translated to humans.

References: [1] Saag et al. (1998) Interstitial Lung Diseases. In: Textbook of Pulmonary Diseases. [2] Beckmann et al. (2002) Am J Physiol Lung Cell Mol Physiol 283:L22-30. [3] Cleveland et al. (2014) NMR Biomed doi:10.1002/nbm.3127. [4] Rinck et al. (1984) Fortschr Röntgenstr 140:239-243. [5] Carrero-Gonzalez et al. (2013) Magn Reson Med 70:1761-1764. [6] Couch et al. (2013) Radiology 269:903-909. [7] Halaweish et al. (2013) Chest 144:1300-1310. [8] Nouls et al. (2011) Concepts Magn Reson B 39B(2):78-88. [9] Ouriadov et al. (2014) Magn Reson Med doi:10.1002/mrm.25406.